Pergamon

Int. J. Heat Mass Transfer. Vol. 39, No. 15, pp. 3157–3164, 1996

0017-9310/96 $15.00+0.00

0017-9310(95)00401-7

Estimation of directional-dependent thermal properties in a carbon–carbon composite

K. J. DOWDING and J. V. BECK
Department of Mechanical Engineering, Michigan State University, East Lansing, MI 48824, U.S.A.

and

B. F. BLACKWELL
Thermophysics Department, Sandia National Laboratories, Albuquerque, NM 87185, U.S.A.

(*Received* 26 *June* 1995 *and in final form* 17 *November* 1995)

Abstract—This paper presents a laboratory method to measure the thermal properties of a carbon–carbon composite material that is characterized by an orthotropic thermal conductivity and isotropic volumetric heat capacity. Thermal properties are estimated using parameter estimation techniques with measured surface heat flux and temperature histories for an experiment with two-dimensional heat flow. Thermal properties were determined for a temperature range of 65–400°C. The thermal conductivity parallel to the fibers is 12–15 times larger than the conductivity normal to the fiber. The results show excellent agreement with separate one-dimensional results, demonstrating a presumed quadratic relationship with temperature.

1. INTRODUCTION

1.1. *Problem description*

Carbon matrix–carbon fiber composite materials have the capability of structural integrity at very high temperatures (>1000°C). In addition, the material has a relatively high thermal conductivity in comparison to other composite materials. These characteristics make the materials well-suited for advanced flight vehicles. Unfortunately, their production and curing processes are not yet consistent in the production of materials that have uniform thermal properties from batch-to-batch. As a consequence, a device for measuring the thermal properties of these materials is needed. This paper further discusses a laboratory method for measuring thermal properties (as a function of temperature and direction) and is a continuation of the one-dimensional work by Dowding *et al.* [1] and Dowding and Beck [2].

Characterization of the thermal properties (thermal conductivity and volumetric heat capacity) for the carbon–carbon material requires multi-dimensional experiments because the material is anisotropic, displaying physical and thermal characteristic that vary with direction in the material. In addition to the typical fiber-matrix construction of a composite, the carbon–carbon material usually has a conversion layer and glass film that protect the composite from oxidation at elevated temperatures. The layer is formed through a process that converts the surface carbon–carbon composite to silicon carbide (SiC). This conversion layer has considerably different thermal properties than the base composite (ref. [3]), which increases the effective anisotropy of the material. For these reasons, a multi-dimensional experiment is performed to determine effective thermal properties that include the base carbon–carbon composite as well as the SiC conversion layer. The effective thermal conductivity is assumed to be orthotropic, varying in directions normal (k_y) and parallel (k_x) to the fiber direction; the volumetric heat capacity is isotropic. The simultaneous estimation of two components of thermal conductivity requires a two-dimensional experiment.

The investigated material is a carbon matrix–carbon fiber material made by Carbon–Carbon Advanced Technologies, Inc. of Fort Worth, Texas. There are six specimens, 3×3 in and 0.375 in thick. (Testing, presented herein, was performed on two of these specimens.) The specimens are described (by the manufacturer) as CC1 2-D composite made from fiberite K-641 fully densified, SiC pack coated with sealant. Because the specimens were not flat as received, the specimens were ground to produce flat surfaces. (During the grinding process a minimal amount of material was removed and the SiC surface was not completely removed.)

1.2. *Motivation*

Interest in the solution of multi-dimensional inverse problems has gained momentum, particularly in recent years. As the importance and wide-spread application of inverse methods are realized, so too have the demands on the complexity of the problems

NOMENCLATURE

C	specific heat [J kg^{-1} °C^{-1}]	Y	measured temperature [°C].
e	temperature residual [°C]		
Fo	Fourier number	Greek symbols	
J	number of temperature sensors	$\boldsymbol{\beta}$	unknown parameter vector
k	thermal conductivity [W m^{-1} °C^{-1}]	δ	thickness of mica heater assembly [m]
L	length [m]	$\boldsymbol{\mu}$	prior information vector
N_t	number of measurement times	ρ	density [kg m^{-3}]
N_p	number of parameters to estimate	Ω	resistance [ohms].
$\dot{q}''$	heat flux [W m^{-2}]		
S	sum-of-squares function		
T	temperature [°C]	Subscripts	
$\hat{T}$	calculated temperature [°C]	cc	carbon–carbon composite material
t	time [s]	Ins	insulating material
$\mathbf{U}$	weighting matrix for prior information	x	direction parallel to the fiber direction
$\mathbf{W}$	weighting matrix for sensors	y	direction normal to the fiber direction.

that can be solved. Such is the case for the application of inverse methods to the field of heat transfer. Two examples are the estimation of the thermal properties of a material and the determination of the heat flux at a boundary, both from experimental measurements. The latter problem is the inverse heat conduction problem (IHCP), which has been the main focus of research on multi-dimensional inverse problems in heat transfer. The application of inverse methods to evaluate the IHCP or estimate thermal properties is closely related, however.

A variety of methods which are used to solve the one-dimensional IHCP, have been extended to the multi-dimensional case. Osman and Beck [4], Hsu *et al.* [5] and Bass [6] use methods based on the function specification method [7]. Murio [8] has presented a mollified space-marching algorithm. The adjoint method is employed by Jarny *et al.* [9] and Truffart *et al.* [10]. Alifanov and Egorov [11], Alifanov and Kerov [12], and Alifanov [13] have presented formulations for iterative regularization methods to solve the two-dimensional problem. The Monte-Carlo method was investigated by Haji-Sheik and Buckingham [14].

Although a great deal of energy has been focused on the multi-dimensional IHCP, less work has been afforded to the estimation of thermal properties using inverse methods for the multi-dimensional case. Loh and Beck [15] performed an experimental investigation for the estimation of thermal properties, orthotropic thermal conductivity and isotropic volumetric heat capacity, in a carbon–carbon composite. Jarny *et al.* [9] formulated the analysis of the thermal conductivity using an adjoint method.

The lack of research on the multi-dimensional estimation of thermal properties may be due to the small number of materials that display an appreciable anisotropy. Due to the construction and advancement of composite materials, however, anisotropic thermal properties are inherent in the composite; the magnitude of the anisotropy depends on the type of materials. For the carbon–carbon material investigated by Loh, the thermal conductivity varied nearly an order of magnitude for directions normal and parallel to the fiber direction. This anisotropic nature of the composite material requires multi-dimensional inverse solution methods to accurately determine the thermal properties. The main contributions of this paper are the application of multi-dimensional inverse methods to actual experimental data to estimate the thermal properties and the determination of these properties over a temperature range of up to 400°C.

Although this paper focuses on a laboratory method, the extension of a method to the field, i.e. while the aircraft is on the runway or in the hanger, is of particular interest for the carbon–carbon material because of the variability that the thermal properties demonstrate. An *in situ* method would also allow changes in the material properties to be tracked during development and operation of the vehicle. The methods presented herein are not easily extended experimentally to a field application due to the practicality of instrumenting the material. What is demonstrated, however, is the applicability of the analysis and algorithms to determine the thermal properties given experimental data. More work on the design and optimization of the experiments is required to move the methods to the field. The authors feel the methods are promising.

2. EXPERIMENTAL ASPECTS

A sketch of the experimental set-up used to estimate the thermal properties of the carbon–carbon material is shown in Fig. 1. It consists of two nominally identical carbon–carbon composite specimens (7.62 × 7.62 × 0.914 cm) and ceramic insulations (7.62 × 7.62 × 2.54 cm, Zircar Products Inc., Florida,

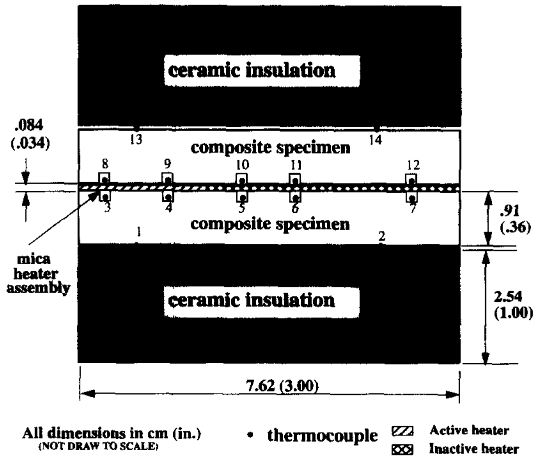

Fig. 1. Schematic of the experimental set-up.

NY) with a mica heater assembly (Thermal Circuits, Inc., Salem, MA., $\Omega(T_{\text{room}}) = 33\ \Omega$) located between the halves. The heater assembly consist of three (2.34×7.62 cm) independently controlled heaters that extend over the entire surface normal to the page for negligible temperature variation in this direction. For two-dimensional experiments, only one of the three heaters is activated. Five thermocouples (Type E, 0.254 mm nom. wire diameter) are embedded on the surface of each carbon–carbon specimen at the heater/specimen interface. The thermocouples (insulation removed) are cemented into grooves (0.381 wide $\times$ 0.457 mm deep) that extend the length of the specimen (normal to the page). Two thermocouples are at each interface of the carbon–carbon specimen and the ceramic insulation. The entire set-up is mounted between two 3.18 mm thick aluminum plates that are connected with threaded rods and hold the layers firmly in place and put in a furnace, which allows the initial temperature to be varied. A detailed discussion of the experimental aspects are given in Ulbrich *et al.* [16].

The thermal experimental model is shown in Fig. 2. All outer surfaces are assumed to be insulated, except for the surface where the energy is introduced by the heater. The energy to the heater is assumed to divide equally between the two halves and emanate from the middle of the heater assembly ($y = -0.042$ cm). The adequacy of the assumed insulated outer surfaces for the model can be verified by a comparison of the natural convection with the anticipated applied heat flux from the heater assembly. Since a temperature rise of 20–25°C above the ambient is expected for a typical experiment and heat loss is mainly due to natural convection ($h \approx 4$ W m^{-2} C^{-1}), these losses are negligible ($\dot{q}'' \approx 100$ W m^{-2}) in comparison to the applied heat flux (see Table 2). Hence, insulated boundary conditions on the outer surfaces are applicable.

The measured temperatures are averaged on opposite sides of the heater assembly to determine the temperature at each location. The locations of the thermocouples are given in Table 1. The sensors that are embedded in the specimen are assumed to measure the temperature at the surface of the specimen. Since ($k_{y,\text{cc}} \gg k_{\text{Ins}}$) small temperature gradients exist in the specimen near the specimen/insulation interface and the non-embedded sensors are assumed to measure the temperature at the backside of the specimen.

Taktak [17] investigated optimal experimental conditions to estimate the orthotropic thermal conductivity for this geometry. However, his model had a temperature boundary condition at the backside of the composite, instead of an (approximate) insulation condition which is used here. Taktak showed that for two sensors, the extremes ($x = 0, 7.62$ cm) on the heated surface ($y = 0$), were optimal for the condition that heating occurred over one-half of the surface. For this case, which is approximately insulated at the backside of the specimen, includes the thermal effects of the heater element, and heats over one-third of the surface, a similar outcome would be expected. Measurement of the temperature on the surface where the heater is active and locations where it is not active provides contrasting effects, which will improve the accuracy of the estimates.

3. ANALYSIS PROCEDURES

The techniques used to estimate the thermal properties are detailed in a book by Beck and Arnold [18]. The basic process involves minimizing a sum of squares function,

$$S = (\mathbf{Y}-\hat{\mathbf{T}})^{\mathrm{T}}\mathbf{W}(\mathbf{Y}-\hat{\mathbf{T}}) + (\boldsymbol{\mu}-\boldsymbol{\beta})^{\mathrm{T}}\mathbf{U}(\boldsymbol{\mu}-\boldsymbol{\beta}) \quad (1)$$

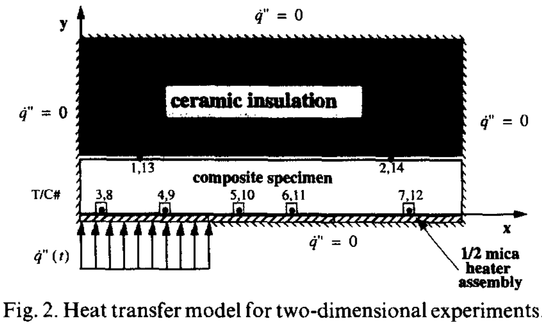

Fig. 2. Heat transfer model for two-dimensional experiments.

Table 1. Sensor locations for two-dimensional experiments

Sensor	Location cm (in) x	y
3,8	0.89(0.35)	0
4,9	1.91(0.75)	0
5,10	3.18(1.25)	0
6,11	4.45(1.75)	0
7,12	6.73(2.65)	0
1,13	1.27(0.5)	L_y
2,14	6.35(2.5)	L_y

Table 2. Thermal properties from two-dimensional analysis for the carbon–carbon composite

Exp. no.	Initial temperature [°C]	r.m.s. [°C]	$k_{x,cc}$ [W m^{-1} C^{-1}]	$k_{y,cc}$ [W m^{-1} C^{-1}]	$\rho C_{cc} \times 10^{-6}$ [J m^{-3} C^{-1}]	Heat flux [s]	[W m^{-2}]
1	65	0.168	58.4	3.89	1.52	80	5276
2	111	0.183	61.0	4.17	1.74	80	6095
3	158	0.163	60.7	4.24	1.93	80	6910
4	205	0.210	61.8	4.55	2.13	80	8905
5	256	0.202	61.6	4.73	2.34	80	8792
6	297	0.295	58.8	4.97	2.36	40	17 304
7	353	0.277	58.7	5.07	2.56	40	17 259
8	403	0.256	57.4	5.09	2.66	40	17 096

where **Y** and $\hat{\mathbf{T}}$ are vectors of the measured and calculated temperatures and **W** is a weighting matrix for the sensors (typically the identity matrix). The last term in equation (1) serves as a regularization or allows for the inclusion of prior information about the thermal properties. It contains the difference between the prior information $\boldsymbol{\mu}$ and present iteration estimates $\boldsymbol{\beta}$ with a weighting matrix **U**. For this analysis no prior information was used. To determine the thermal properties the function S is minimized with respect to the thermal properties ([18], equation 7.4.6).

The computer program PROP2D implements this inverse method to determine the two-dimensional properties. The program was developed at Michigan State University by taking the finite element code TOPAZ2D (Shapiro [19]) and combining this direct problem solver with these parameter estimation methods, to create a powerful algorithm. PROP2D allows for the estimation of the thermal properties for multiple materials, with irregular geometries allowable, from transient temperature and heat flux histories. The thermal conductivity can be orthotropic and temperature dependent thermal properties are possible.

4. RESULTS AND DISCUSSION

A separate, independent set of one-dimensional experiments (Dowding and Beck [2]) was performed to determine the thermal properties of the mica heater and ceramic insulation in the model (Fig. 2). Effective properties were determined to account for the contact conductance between the layers. Therefore, only the thermal properties of the carbon–carbon composite are unknown in the model (Fig. 2). Furthermore, one-dimensional experiments were performed to determine the thermal conductivity normal to the fibers ($k_{y,cc}$) and the volumetric heat capacity (ρC_{cc}) (Dowding *et al.* [1] and Dowding and Beck [2]). The one-dimensional results provide initial estimates for the two-dimensional analysis and allow for a comparison to demonstrate the accuracy and consistency of the methods.

For the two-dimensional experiments, the analysis is more sensitive to the experimental conditions. For example, the magnitude and duration of the heat flux must produce adequate response (sensitivity coefficients) for the sensors nearer to the active heater, as well as for the sensors further from the active heater. This requires a longer heating duration than that used for the one-dimensional experiments. The locations of the thermocouples must also be known accurately, especially on the active heater where large temperature gradients exist. Although it is not too difficult to locate the position of the thermocouples in the carbon–carbon specimen, it is difficult to align the mica heater assembly relative to the specimens, since the heating elements are not visible in the heater assembly.

The two-dimensional thermal properties of the carbon–carbon composite determined for temperatures up to 400°C are given next. Experiments were conducted at regular intervals over this temperature range and analyzed assuming the thermal properties were constant for the duration of an experiment, but varied between experiments. The measured experimental data and details of the parameter estimation are presented and briefly discussed for a typical experiment.

4.1. *Experimental data*

Experimental data for a test started at a temperature of 297°C (experiment case 6) are shown in Fig. 3. A sampling interval of 0.64 s is used to acquired data for this experiment. The heating begins at approximately 16 s and ends at 56 s. For experiments at lower initial temperatures the heating duration was 80 s. However, based on observation of the sensitivity coefficients and the criteria for optimal experiments, 'D-optimality' (Chap. 8, ref. [18]), a shorter duration, higher magnitude heat flux was selected to be closer to the optimal experimental conditions for determining the two components of the thermal conductivity and the volumetric heat capacity.

The effect of the orthotropic thermal conductivity is seen by comparing the temperature rise for the sensors at $x = 3.81$ cm on the heated surface (sensors 5, 10) and $x = 1.27$ cm on the insulated surface (sensors, 1, 13). The larger thermal conductivity in the x-direction results in a nearly instantaneous response at $x = 3.81$ cm on the heated surface, while the sensor at $x = 1.27$ cm on the insulated surface has approximately a 4 s time delay before responding. This delay

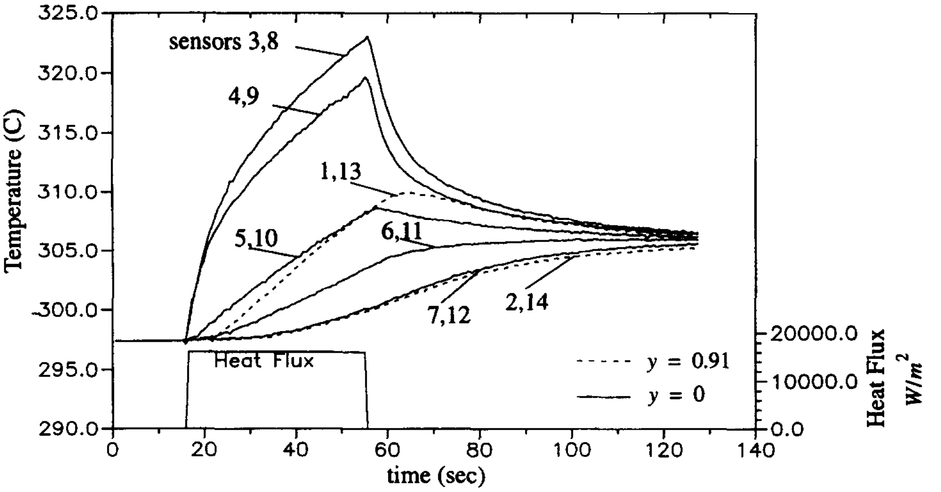

Fig. 3. Experimental data for experiment begun at $T = 297$°C (experiment 6).

exists, even though the sensors are approximately the same distance from the active heater (~10% difference, 0.835 and 0.914 cm from the sensor on the heated surface and insulated surface, respectively).

Notice that the temperature data are acquired after the heating ends. Continuing to acquire data after stopping the heat flux will result in better estimates. This is because it causes the sensitivity coefficients to be of different shape from one another after heating. These effects result in a more accurate estimation of multiple thermal properties based on the criteria 'D-optimality with constraints' (p. 459, ref. [18]). Possible heat losses in the experimental set-up can also be monitored with this data, although it does not appear that there are significant losses in this experiment, since all temperature sensors are converging towards a constant.

4.2. *Estimated thermal properties*

For two-dimensional analysis, as compared to the one-dimensional, the numerical issues are more important. The mesh size and time step selected for the finite element method can greatly influence the amount of time required to obtain a solution and the accuracy of this solution. The mesh used for this analysis contains 525 (quadrilateral) elements. Along the 7.62 cm surface (x-direction) there are 25 elements for all materials. There is one element across the mica heater assembly and 10 elements across each the carbon–carbon specimen and ceramic insulation (y-direction). The computational time step chosen was 0.64 s, the same as the experimental time step. A typical two-dimensional analysis required 2–4 h on a VAXstation 4000 Model 60 running VMS V5.5-2, depending on the number of iterations and accuracy of the initial parameter estimates; typically four to five iterations (16–20 direct solutions) were required. Although a detailed investigation was not performed, the time step and mesh size were varied and shown to have little influence on the resulting estimated thermal properties.

The two-dimensional thermal properties determined for the carbon–carbon composite are summarized in Table 2. The experiment case number and initial temperature are given in columns one and two. The next four columns present the root-mean-square (r.m.s.) and the two-dimensional thermal properties determined from the analysis. The final two columns give the duration and magnitude of the applied heat flux. A plot of each of the thermal properties ($k_{x,cc}$, $k_{y,cc}$, and ρC_{cc}) as a function of the initial temperature is shown in Fig. 4. An F-test (ref. [18]) indicated a second-order model (in temperature) for these properties. Because limited results are available, the relationship for $k_{x,cc}$ remains linear. The relationships determined with a least square fit, are shown in Fig. 4 and given by the following relationships (T in °C):

$$k_{y,cc} = 3.470 + 0.00653T - (0.593 \times 10^{-5})T^2 \quad (2)$$

$$k_{x,cc} = 61.209 - 0.00614T \quad (3)$$

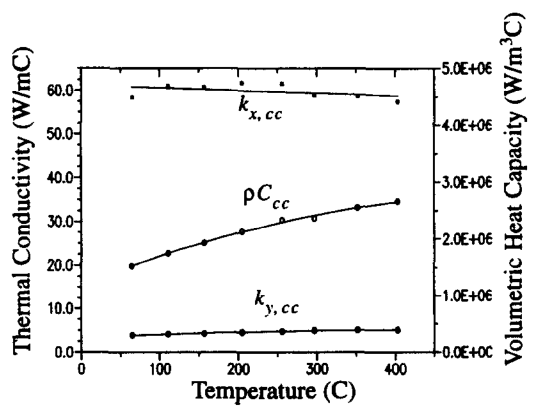

Fig. 4. Estimated thermal properties for two-dimensional analysis.

$$\rho C_{cc} = [1.188+0.00549T-(0.460\times 10^{-5})T^2]\times 10^6. \quad (4)$$

The thermal conductivity parallel to the fibers ($k_{x,cc}$) is 12–15 times as large as that normal to the fibers ($k_{y,cc}$). Testing was halted at 400°C due to the failure of the carbon–carbon specimen during subsequent one-dimensional testing at higher temperatures.

In addition to estimating the thermal properties, PROP2D provides some means to quantify the accuracy of the estimates. The r.m.s., which is given in Table 2, provides an indication of how well the calculated temperatures match the experimentally measured temperatures. The magnitude of the r.m.s. can be compared to the temperature rise of the experiment, which is approximately 25°C. The r.m.s. is within 1.2% of the maximum temperature rise for all the experiments and many are less than 1%. The r.m.s. is largest for the last three experiments, which applied a larger heat flux for a shortened duration.

There are other quantities that can be observed to demonstrate the accuracy of the estimated properties. These quantities are the sequential estimates of the thermal properties and the temperature residuals. Each is discussed below for experiment 6.

The sequential estimates demonstrate how the estimated properties vary as additional experimental measurements are considered. Figure 5 shows the sequential estimates for this experiment. The sequentially estimated property, at time t_i, represents the outcome if only data up to that time is used in the analysis. In other words, if the data is analyzed by adding one data set at each time, it shows how the estimated properties change as one more data set is added to the analysis. Initially the sequential estimates vary because there is not enough information (data) to accurately determine the properties. However, as more data is considered, the property estimates approach constants. If the experiment (or analysis) is ended at 80 s, the estimated properties would not differ significantly from the properties at 100 s. In general, for a good estimation the sequential estimates converge to a constant and are steady with time. For this experiment the sequential estimates for $k_{x,cc}$, $k_{y,cc}$, and ρC_{cc} vary only 2.8, 1.4 and 0.8% over the final 48 s (80–128 s) of the experiment.

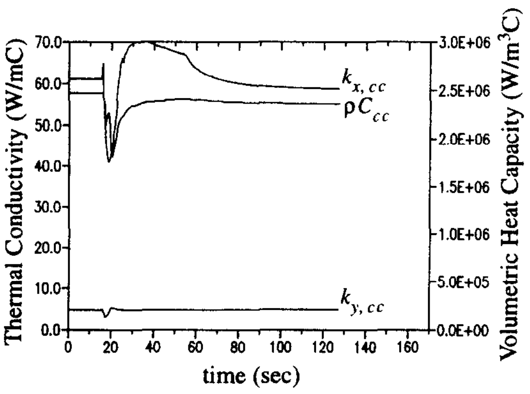

Fig. 5. Sequential parameter estimates for experiment begun at $T = 297$°C (experiment 6).

The temperature residuals are related to the r.m.s. and are calculated as follows:

$$e_{ii} = Y_{ii} - \hat{T}_{ii}. \quad (5)$$

They represent the difference between the measured and calculated temperature for a particular time (t_i) and sensor location (x_j, y_j). The r.m.s. gives an indication of the magnitude of the residuals; the sign and magnitude of the individual residual can provide considerable insight. The residuals for this experiment, 6, are shown in Fig. 6(a–c). Figure 6(a) presents the residuals for the sensors on the active heater, Fig. 6(b) the residuals for the sensors on the heated surface,

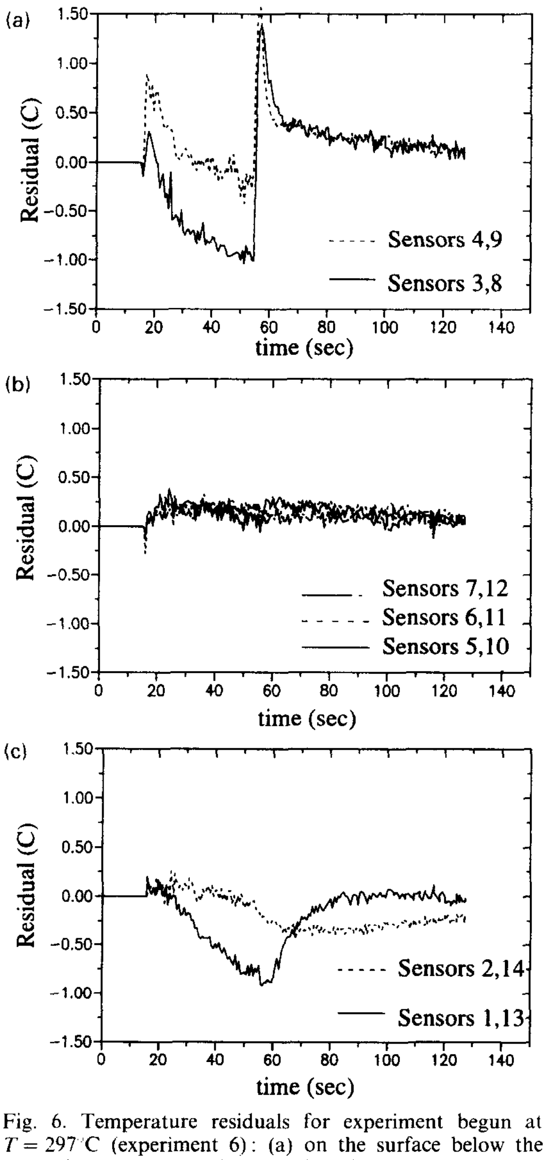

Fig. 6. Temperature residuals for experiment begun at $T = 297$°C (experiment 6): (a) on the surface below the active heater; (b) on the heated surface, but not on the area of the active heater; and (c) at the specimen/insulation interface.

but not on the active heater, and Fig. 6(c) the residuals for the sensors at the insulated surface. The residuals for the sensors on the heated surface, but not on the active heater [Fig. 6(b)], are slightly correlated. The other residuals, Fig. 6(a–c), are highly correlated and larger, 4–5% of the temperature rise on the heated surface and 8–10% of the temperature rise at the insulated surface. It is not clear exactly why the residuals are so highly correlated. Two possible reasons are the uncertainty in the location of the sensors with respect to the heater and a non-uniform heat flux produced by the heater. There is some uncertainty in the alignment of the heater assembly and the specimen. The heating elements are contained within an opaque fiberglass with a mica layer on the outside. Since the fiberglass and mica extend beyond the heating elements, the alignment of the edge of the heater (element) with the specimen is difficult. Secondly, the design of the heating element has a gap between successive coils allowing for areas of localized heating. If the sensors align with a gap, the actual heat flux will be larger than that calculated flux, which assumes a uniform profile. Similarly, the sensors aligned with the heating element will have a larger heat flux than the calculated uniform flux. The residuals for sensors away from the active heater are less sensitive to the location and uniformity of the heat flux and therefore, are less affected.

To investigate the correlated residuals, two numerical experiments are conducted. The first experiment had an error in the location of the heater and the second had a non-uniform heat flux; no other measurement errors are present. These experiments were analyzed assuming no error in the location of the heater and a uniform heat flux to investigate the effect on the residuals. Unfortunately, the results of these numerical experiments were not conclusive. In particular, the two errors had opposite effects on the residuals. An error in the location of the heater resulted in a residual that had an opposite sign to the residuals for a non-uniform heat flux. The shapes of the residual curves for the numerical experiments were quite different from the experimental case (Fig. 6), especially for sensors not at the location of the applied heat flux.

4.3. *Comparison to one-dimensional results*

As mentioned previously, in addition to the two-dimensional experiments, one-dimensional experiments [1] were conducted and results for the thermal conductivity normal to the fiber and the volumetric heat capacity were obtained. The results obtained for one-dimensional analysis were used as initial estimates for the two-dimensional analysis; however, the thermal properties were not constrained in the two-dimensional analysis using the one-dimensional results.

The properties determined from the one- and two-dimensional experiments are compared in Fig. 7(a, b). Overall, the results are quite close. The two-dimensional results are slightly higher for $k_{y,cc}$ and slightly

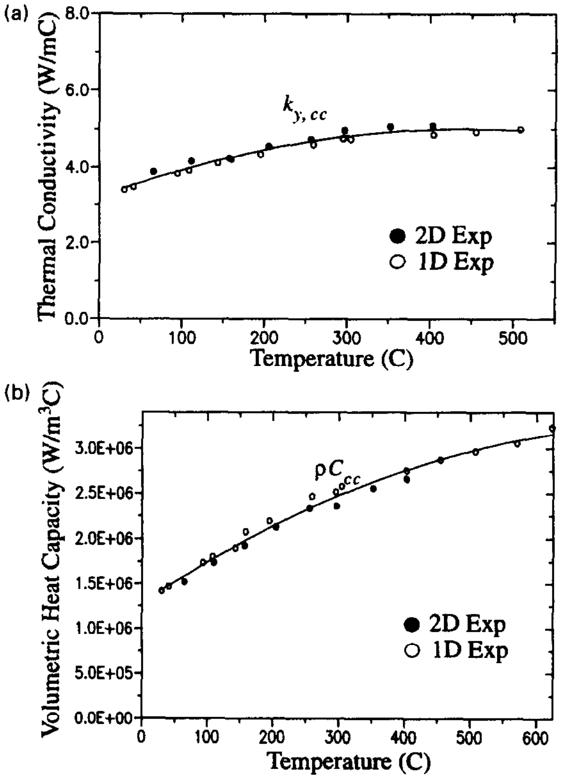

Fig. 7. Comparison of one- and two-dimensional estimated thermal properties: (a) thermal conductivity $k_{y,cc}$; and (b) volumetric specific heat ρC_{cc}.

lower for ρC_{cc}. Recall that the properties were estimated assuming they were constant over the duration of an experiment and therefore are applicable for a 20–25°C temperature range. Noting this, the one and two-dimensional estimates for $k_{y,cc}$ are within 6%, with the largest errors at the higher temperatures where limited two-dimensional data is available. There is also a dip downward for the estimates near the maximum temperature, an unexpected result that may indicate the thermal conductivity is approaching a constant, but more testing (at higher temperatures) is needed to verify. The results for ρC_{cc} have a maximum of 7% deviation between the one- and two-dimensional estimates.

The temperature dependence determined using both one- and two-dimensional results, which were also indicated to be second order in temperature using a F-test, are

$$k_{y,cc} = 3.217+0.00808T-(0.915\times10^{-5})T^2 \quad (6)$$

$$\rho C_{cc} = [1.284+0.00487T-(0.299\times10^{-5})T^2]\times10^6. \quad (7)$$

The relationship for $k_{x,cc}$ has only two-dimensional results and is given by equation (3). The estimated thermal properties, from both one- and two-dimensional experiments, are within 4% and 6% of the relationships given in equations (6) and (7) for $k_{y,cc}$ and ρC_{cc}.

5. SUMMARY AND CONCLUSIONS

A laboratory method to measure the thermal properties of carbon matrix–carbon fiber composite material was presented. Thermal properties were calculated using parameter estimation techniques for the carbon–carbon composite from two-dimensional experiments using measured temperature and heat flux histories.

The analysis methods and algorithms were very powerful; two components of thermal conductivity ($k_{x,cc}$, $k_{y,cc}$) and the volumetric heat capacity were simultaneously determined with two-dimensional experiments for temperatures up to 400°C. The thermal properties estimated with two-dimensional experiments vary 6–7% from the thermal properties estimated using one-dimensional experiments.

Acknowledgements—This work was performed at Michigan State University and Sandia National Laboratories under US Air Force contract number FY1456-91-N0058. This research was also partially supported by the Research Excellence Fund of the State of Michigan through the Composite Materials and Structures Center at Michigan State University. Most of the experimental work was performed by Arthur Ulbrich. The input of Jim Hayes at Wright–Patterson Air Force Base is acknowledged.

REFERENCES

1. K. Dowding, J. Beck, A. Ulbrich, B. Blackwell and J. Hayes, Estimation of thermal properties and surface heat flux in a carbon–carbon composite material, *J. Thermophys. Heat Transfer* **9**, 345–351 (1995).
2. K. J. Dowding and J. V. Beck, Measurements of transient temperatures and heat fluxes in a composite material for the estimation of thermal properties—part II: property determination and heat flux estimation, technical report MSU-ENGR-004-94, Michigan State University, East Lansing, MI, February (1994).
3. F. P. Incropera and D. P. DeWitt, *Introduction to Heat Transfer* (2nd Edn), Appendix A. Wiley, New York (1990).
4. A. M. Osman and J. V. Beck, Investigation of transient heat transfer coefficients in quenching experiments, *J. Heat Transfer* **112**, 843–848 (1990).
5. T. Hsu, N. G. Sun, Chen and Z. Gong, Finite element formulation for two-dimensional inverse heat conduction analysis, *J. Heat Transfer* **114**, 553–557 (1992).
6. B. R. Bass, Application of the finite element method to the nonlinear inverse heat conduction problem using Beck's second method, *J. Heat Transfer* **102**, 168–176 (1980).
7. J. V. Beck, B. Blackwell and C. R. St. Clair Jr, *Inverse Heat Conduction: Ill-posed Problems*, Chap. 5. Wiley, New York (1985).
8. D. Murio, On the numerical solution of the two-dimensional inverse heat conduction problem by discrete mollification, *Proceedings of Inverse Problems in Engineering: Theory and Practice*, ASME, Florida, pp. 17–21 (1993).
9. Y. Jarny, N. M. Ozisik and J. P. Bardon, A general optimization method using adjoint equation for solving multidimensional inverse heat conduction, *Int. J. Heat Mass Transfer* **34**, 2911–2919 (1991).
10. B. Truffart, Y. Jarny and D. Delaunay, A general optimization algorithm to solve 2-D boundary inverse heat conduction problems using finite elements, *Proceedings of Inverse Problems in Engineering: Theory and Practice*, ASME, Florida, pp. 53–60 (1993).
11. O. M. Alifanov and Y. V. Egorov, Algorithms and results of solving the inverse heat conduction problem in a two-dimensional formulation, *J. Engng Phys.* **48**, 489–496 (1985).
12. O. M. Alifanov and N. V. Kerov, Determination of external thermal load parameters by solving the two-dimensional inverse heat-conduction problem, *J. Engng Phys.* **41**, 1049–1053 (1981).
13. O. M. Alifanov, *Inverse Heat Transfer Problems*. Springer, New York (1994).
14. A. Haji-Sheikh and F. Buckingham, Multi-dimensional inverse heat conduction using the Monte Carlo method, *J. Heat Transfer* **115**, 26–33 (1993).
15. M. Loh and J. V. Beck, Simultaneous estimation of two thermal conductivity components from transient two-dimensional experiments, paper 91-WA/HT-11 presented at ASME Winter annual meeting, Atlanta, GA (1991).
16. A. Ulbrich, J. V. Beck and K. Dowding, Measurements of transient temperatures and heat fluxes in a composite material for the estimation of thermal properties—part I: experimental aspects, technical report MSU-ENGR-009-93, Michigan State University, East Lansing, MI (1993).
17. R. Taktak, Design and validation of optimal experiments for estimating thermal properties of composite materials, Ph.D thesis, Michigan State University, East Lansing, Michigan (1992).
18. J. V. Beck, and K. J. Arnold, *Parameter Estimation in Engineering and Science* (1st Edn). Wiley, New York (1977).
19. A. B. Shapiro, *TOPAZ2D A Two-Dimensional Finite Element Code For Heat Transfer Analysis, Electrostatic, and Magnetostatic Problems*. Lawrence Livermore National Laboratory, CA (1986).